JMM Journal of Menopausal Medicine
pISSN: 2288-6478, eISSN: 2288-6761
https://doi.org/10.6118/jmm.23015
J Menopausal Med 2024;30:104-119
ORIGINAL ARTICLE

Effects and Mechanism of AP39 on Ovarian Functions in Rats Exposed to Cisplatin and Chronic Immobilization Stress

Ebru Onalan[1], Bilgi Erbay[2], İlay Kavuran Buran[1], Deniz Erol[3], Ahmet Tektemur[1], Tuncay Kuloglu[4], Ibrahim Hanifi Ozercan[5]

[1]Department of Medical Biology, Faculty of Medicine, Firat University, Elazığ, Türkiye, [2]School of Molecular and Cellular Biology, Faculty of Biological Sciences, University of Leeds, Leeds, UK, [3]Department of Medical Genetics, Faculty of Medicine, Firat University, Elazığ, Türkiye, [4]Department of Histology and Embryology, Faculty of Medicine, Firat University, Elazığ, Türkiye, [5]Department of Pathology, Faculty of Medicine, Firat University, Elazığ, Türkiye

Objectives: Premature ovarian failure (POF) rat models are essential for elucidating the hormonal and ovarian molecular mechanisms of human POF diseases and developing new therapeutic agents. This study aimed to compare the applicability of chronic immobilization stress (CIS) as a POF model with that of cisplatin and to examine the impact of AP39, a mitochondrial protective agent, on ovarian function in rats treated with cisplatin and CIS.

Methods: Sixty Sprague–Dawley female rats were divided equally into six groups (10 per group): Control, Cisplatin, AP39, Cisplatin + AP39, CIS, and CIS + AP39. Ovarian dysfunction was induced with cisplatin (3 mg/kg) or CIS. Forced swim test, hormone concentrations, estrous cyclicity, histopathology, follicle counts, and molecular alterations in the ovary and mitochondria were analyzed.

Results: In the CIS and cisplatin groups, mitochondrial biogenesis, egg quality, hormonal profile, estrous cycle, and folliculogenesis significantly declined. Nonetheless, most of the parameters with undesirable results did not normalize after AP39 administration.

Conclusions: The cisplatin- and CIS-treated rats exhibited unshared deteriorated hormonal pathways and similarly disrupted gene expression patterns. Our current CIS model did not meet the human POF criteria, which include decreased estradiol levels, despite having advantages in terms of ease of modeling and reproducibility and demonstrating pathological changes similar to those observed in human POF. Therefore, rather than using this model as an POF model, using it as a representation of stress-induced ovarian dysfunction would be more appropriate.

Key Words: AP39, Chronic immobilization stress, Cisplatin, Premature ovarian failure

INTRODUCTION

Roughly 1% of female under 40 experience premature ovarian failure (POF), also referred to as the depletion of oocytes in the ovaries before to menopause for a variety of causes [1]. The causes of POF, which is highly heterogeneous, include iatrogenic (bilateral oophorectomy, chemotherapy, and radiation) as well as autoimmune, inflammatory, metabolic, infectious, and stress-related conditions [2].

Ovarian tissue is harmed by the excessive generation of reactive oxygen species brought on by severe mitochondrial depletion and disturbances in mitochondrial biogenesis, according to the molecular ovarian processes of POF. Ovarian reserve and oocyte quality are reduced to varying degrees depending on the conditions that lead to polycystic ovary syndrome, including chemotherapeutic drugs and stress [3,4]. Although some of the treatments are still experimental, it has been established that certain medicines and mitochondrial protective molecules are efficient inhibitors of chemotherapy-induced ovarian damage in POF [5-7]. A hydrogen sulfide (H_2S) donor that targets mitochondria, AP39 [(10-oxo-10-(4-(3-thioxo-3H-1,2-dithiol-5-yl) phenoxy) decyl) triphenylphosphonium bromide], demonstrated protective benefits against oxidative

Received: June 12, 2023 **Revised:** August 2, 2024 **Accepted:** August 3, 2024
Address for Correspondence: İlay Kavuran Buran, Department of Medical Biology, Faculty of Medicine, Firat University, Elazig 23119, Türkiye
Tel: 90-424-2370000/4646, **E-mail:** iburan@firat.edu.tr, **ORCID:** https://orcid.org/0000-0002-2890-3952

stress and mitochondrial dysfunction in vitro [8].

Once thought to be a poisonous gas, H_2S is actually a small molecule that conducts gases. It is either released from pharmacologic vehicles or made very little endogenously. The molecule participates in the pathogenesis of several disorders, including arteriosclerosis and heart attacks, and possesses intracellular messenger and neuromodulatory properties. H_2S predominantly targets mitochondria, where it modifies the electron transport system in a dose-dependent fashion. Through irreversible oxidation by the enzyme sulfite-quinone oxidase, it functions as an electron donor at low concentrations in the electron transport chain (ETS). The electrons from the oxidation of H_2S enter the ETS system through complex III, which increases oxidative phosphorylation and ATP synthesis [9-11]. H_2S metabolism is increased to protect mitochondria from oxygen and glucose deprivation. However, concentrations higher than 50 μM can inhibit ETS, leading to redox imbalance, inhibition of cell division, and a shift in metabolism towards reductive carboxylation [12]. The therapeutic and protective effects of AP39 in rodent models of hypertension, diabetes, renal ischemia/reperfusion (I/R), myocardial I/R, and APP/PS1 Alzheimer's disease are associated with its anti-inflammatory, anti-apoptotic, anti-oxidant, and anti-fibrotic mechanisms [8,13-16].

A range of therapeutic approaches, focusing on iatrogenic, environmental, and genetic factors, have been tried to prevent and cure the symptoms of POF. Furthermore, many characteristics have been used to construct animal models of POF in order to support therapeutic studies. Criteria for model construction and success have been applied specifically to benchmarks such ovarian injury, ovarian follicle maturation, and hormone alterations. There are notable variations in dosage and model creation time even in the animal model of POF produced by cisplatin. These limitations have led to the lack of a standard for POF animal models induced by various drugs or causes. Therefore, selecting appropriate animal models for researching treatment methods for POF remains a challenge for researchers [6]. Due to these reasons, there is still no standard for POF animal models induced by different agents or factors. An animal model known as the chronic unpredictable mild stress (CUMS) POF is frequently used to assess ovarian dysfunction brought on by psychological stress [17]. In contrast to CUMS, immobilization or restraint stress is also a frequently employed experimental model for evaluating the physiological reactions to stress and the anti-stress properties of pharmaceutical drugs in small rodents. It is considered more convenient and less painful [18]. It is thought to be less uncomfortable and more convenient. Although a study has demonstrated the effects of chronic restraint stress on mice ovaries, chronic immobilization stress (CIS) as a model for ovarian dysfunction or a point-of-failure stress paradigm has not yet undergone a thorough examination [19]. In rats treated with cisplatin or CIS as POF models, the correcting effects of an oxidant damage-alleviator of AP39 have not yet been examined.

In a single study evaluating the therapeutic effects of mitochondria-protective agents in rodent models of POF, administration of CoQ10, a mitochondrial-protective agent that transports electrons from complexes I and II to complex III, was shown to successfully reverse cyclophosphamide-induced ovarian damage [5]. The aim of this study was to evaluate the feasibility of long-term CIS treatment as a POF model in female rats by comparing it with the traditional cisplatin rat model, to identify the morphological, hormonal and ovarian molecular components responsible for female reproductive system defects in cisplatin and CIS rat ovarian dysfunction models and to reveal the potential protective effects of AP39, a mitochondrial-protective agent.

MATERIALS AND METHODS

Animals

The present study commenced after the approval of the Firat University Animal Experiments Ethics Committee on 05.05.2017 (No: 9/122). Sixty Sprague-Dawley female rats (320–330 g) were procured from Firat University Experimental Research Center (FUDAM). Rats were housed under standard conditions, a controlled environment with free access to food and water ad libitum.

Experimental design, premature ovarian failure model establishment, and AP39 therapy

Vaginal smear analysis was performed on rats daily for 10 days to screen the estrous cycle (once at 9:00 a.m. every day) before starting applications. Sixty female rats with normal estrus cycles (defined as 4–6 days) were included in the study. The scanned animals were randomly divided into the following six groups of ten animals each: Control, Cisplatin, AP39, Cisplatin + AP39, CIS, and CIS + AP39. Although the apparatus used for

CIS application in rodents is standardized, there are significant differences between studies in terms of the daily application time (3–6 hours) and application duration (1–10 weeks). It is generally accepted that a CIS application of 6 hours a day for approximately 4 weeks is sufficient for the emergence of depressive-like behaviors in rodents [20]. But in our study, the length of the CIS application varied gradually from one hour to three hours, therefore an experimental period of eight weeks was selected, which is a little longer than the recommended term. The experiments were completed in 55 days in the CIS groups and 25 days in the cisplatin groups. CIS protocol was applied to the CIS groups for 55 days. Cisplatin (Kocak Chemical Industry) treatment groups received daily intraperitoneal injections of cisplatin (3 mg/kg/day) for 10 days [7]. Intraperitoneal injection of AP39 (Cayman Chemical Company) at a dose of 0.3 mg/kg/day in phosphate buffer saline solution was administered intraperitoneally on the 11–55th days in CIS + AP39 group or 11–25th days in the Cisplatin + AP39 group [13]. The study protocol and the timelines of applications and therapies are outlined in Figure 1. The body heights and weights of the rats were recorded at the beginning and end of the experiments.

Forced swim test procedures

The experiment was carried out on two consecutive days 15 minutes on the 54th day and 5 minutes on the 55th day of the study. During the total time, a video was recorded to calculate the parameters of the rats' immobility, swimming, and climbing.

Decapitation, blood, and tissue collection

According to the vaginal smear analysis after the applications, the animals with the estrus cycle were sacrificed at the proestrus stage (within 1–3 days after forced swim test [FST]) and those without the cycle were sacrificed on the 55th day by decapitation. Blood samples were collected into centrifuge tubes containing aprotinin and centrifuged at 3,000 g for 10 minutes and the supernatant serums were separated. Ovarian tissues were dissected, weighed, and then divided into two portions for histopathological and real-time polymerase chain reaction analysis. All samples were stored at –80°C until the day of the study.

RNA isolation and quantitative real–time polymerase chain reaction analysis

Total RNA isolation in ovarian tissue was conducted with the "Tri Reagent" protocol (Bioshop) with Turbo DNA-free (Ambion Inc.) DNase treatment. The RNA purity and concentration were measured with a MaestroNano Spectrophotometer at 260 nm (MaestroGen). The cDNA amplification was carried out in a thermal cycler (Applied Biosystems) with an Applied Biosystems High Capacity RNA-cDNA Kit (Applied Bio-

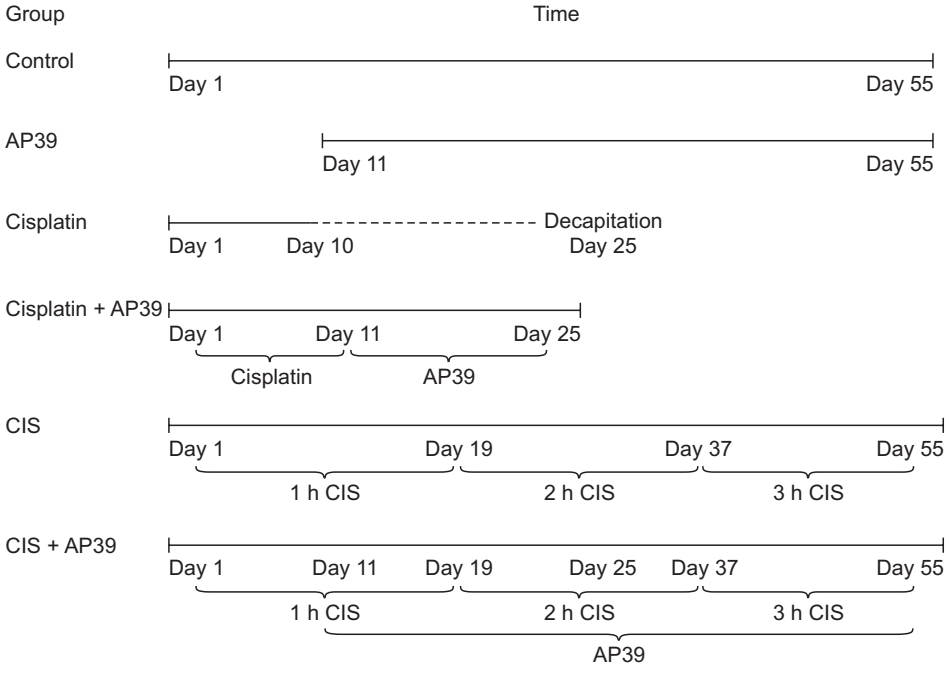

Fig. 1. The schemes of experimental applications in the study groups. The animals were divided equally into six groups of Control, Cisplatin, AP39, Cisplatin + AP39, CIS, and CIS + AP39 (n = 10). The experiments were completed in 55 days in the CIS POF model groups and 25 days in the cisplatin POF model groups. The rats were kept in the immobilization apparatus for 1 hour during the initial 19 days, 2 hours during the next 18 days, and 3 hours during the remaining 18 days. AP39 was administered ip. on the 11–55th days or 11–25th days depending on the AP39 treatment groups. CIS: chronic immobilization stress, POF: premature ovarian failure.

Table 1. Catalog numbers of primers used for quantitative real-time polymerase chain reaction and characteristics of genes related to folliculogenesis and mitochondria

Symbol	Locus	Feature	Qiagen Cat no.
Mitochondrial related genes			
ATP5B (ATP synthase subunit beta, mitochondrial)	12q13.3	Encodes the β subunit of mitochondrial ATP synthase that catalyzes ATP synthesis	PPR53179A
PPARGC1A (PPARG coactivator 1 alpha)	12q13.3	It is a transcriptional coactivator that regulates genes involved in energy metabolism	PPR46783A
PPARGC1B (PPARG coactivator 1 beta)	5q32	It is a transcriptional coactivator that regulates genes involved in energy metabolism	PPR51585A
PRKAA2 (Protein kinase AMP- activated catalytic subunit alpha 2)	1p32.2	It is a catalytic subunit of AMPK that is activated in response to cellular metabolic stresses and regulates fatty acid and cholesterol biosynthesis	PPR51543A
MNF2 (Mitofusin 2)	1p36.22	A mitochondrial membrane protein that participates in mitochondrial fusion and contributes to the maintenance and operation of the mitochondrial network	PPR46301A
OPA1 (Mitochondrial dynamin like gtpase)	3q29	An inner mitochondrial membrane protein that helps regulate mitochondrial stability and energy output	PPR44137A
HIF1 (Hypoxia inducible factor 1)	14q23.2	It is a transcriptional activator of many genes associated with adaptation to low oxygen pressure	PPR44480A
CHRM1 (Cholinergic receptor muscarinic 1)	11q12.3	It is a member of the metabotropic G protein-coupled receptor (GPCR) family and its loss leads to a decrease in mitochondrial respiration (oxygen consumption)	PPR52433A
TFAM (Transcription factor A, mitochondria 1)	10q21.1	A mitochondrial transcription factor involved in mitochondrial DNA replication and repair	PPR06806A
NFE2L2 (Nuclear factor, erythroid 2 like 2)	2q31.2	A transcription factor that regulates genes containing antioxidant response elements	PPR46611A
NRF1 (Nuclear respiratory factor 1)	7q32.2	It is a transcription factor that regulates nuclear genes required for respiration, heme biosynthesis and mitochondrial DNA transcription and replication	PPR45094A
Ovarian and folliculogenesis related genes			
DPPA3 (Developmental pluripotency associated 3)	12p13.31	It is a maternally-acting protein involved in the preimplantation stage and plays a role in transcriptional repression, cell division and maintenance of cell pluripotency	PPR52161A
FIGLA (Folliculogenesis specific bhlh transcription factor)	2p13.3	It is a transcription factor that regulates a large number of oocyte-specific genes. Mutations in this gene cause premature ovarian failure	PPR75855A
DAZL (Deleted in azoospermia like)	3p24.3	The *DAZ* gene family encodes potential RNA-binding proteins expressed in prenatal and postnatal germ cells of male and female	PPR68946B
ZP1 (Zona pellucida glycoprotein 1)	11q12.2	It is a structural component of the zona pellucida and mutations in the gene cause oocyte maturation defects and infertility	PPR45105A
ZP2 (Zona pellucida glycoprotein 2)	16p12.3–p12.2	It is a structural component of the zona pellucida and functions in the secondary attachment and penetration of spermatozoa that react with the acrosome	PPR45106A
POU5F1 (Pou class 5 homeobox 1)	6p21.33	A transcription factor that plays an important role in embryonic development and pluripotency	PPR59727A
NPM2 (Nucleoplasmin 2)	8p21.3	Nucleoplasmin (NPM) chaperone families [NPM1, NPM2, NPM3] have diverse functions in cellular processes such as chromatin remodeling, genome stability, ribosome biogenesis, DNA duplication and transcriptional regulation	PPR59674A
H1FOO (H1 histone family member O oocyte specific)	3q22.1	An oocyte-specific H1 histone involved in chromatin network remodeling	PPR66654A
DNMT1 (DNA methyltransferase 1)	19p13.2	It is an enzyme that binds methyl groups to cytosine nucleotides of genomic DNA and is involved in the repression of gene expression	PPR43733A

Table 1. Continued

Symbol	Locus	Feature	Qiagen Cat no.
DNMT3A (DNA methyltransferase 3 alpha)	2p23.3	It encodes a DNA methyl transferase thought to function in de novo methylation. The protein is localized to the cytoplasm and nucleus and its expression is developmentally regulated	PPR50580A
DNMT3B (DNA methyltransferase 3 beta)	20q11.21	It is a DNA methyl transferase that functions in de novo methylation	PPR59417B
KAT2A (Lysine acetyltransferase 2A)	17q21.2	It is a histone acetyltransferase (HAT) that functions as a transcriptional activator	PPR50679A
HDAC3 (Histone deacetylase 3)	5q31.3	It has histone deacetylase activity and represses transcription	PPR46455B
SIRT7 (Sirtuin 7)	17q25.3	Class III is a member of the histone deacetylase (HDAC) family	PPR47517A
MBD2 (Methyl-cpg binding domain protein 2)	18q21.2	It functions as a demethylase in the methylation process	PPR43331B
KMT2A (Lysine methyltransferase 2A)	11q23.3	It is a transcriptional coactivator involved in regulating gene expression	PPR51308A
SMARCA1 (SWI/SNF related, matrix associated, actin dependent regülatör of chromatin, subfamily a, member 1)	Xq25–q26.1	It is a member of the SWI/SNF protein family and is an ATPase that contributes to the chromatin remodeling complex	PPR49160A
ESR1 (Estrogen receptor 1)	6q25.1–q25.2	The receptor is a ligand-activated transcription factor consisting of several regions important for hormone binding, DNA binding and transcription activation	PPR44939B
GTF2H1 (General transcription factor II H subunit 1)	11p15.1	It is a transcription factor subunit that in many cases regulates transactivation	PPR47902A
MAP2K1 (Mitogen- activated protein kinase kinase 1)	15q22.31	It is a member of the protein kinase family and is involved in many cellular processes such as proliferation, differentiation, transcription regulation and development	PPR43465A
NCOA1 (Nuclear receptor coactivator 1)	2p23.3	It is a transcriptional coactivator for steroid and nuclear hormone receptors	PPM04655A
TBP (TATA-box binding protein)	6q27	A transcription factor that binds to the TATA sequence, which controls the initiation and rate of transcription	PPR47412A
MED15 (Mediator complex subunit 15)	22q11.21	A transcriptional coactivator involved in RNA polymerase II transcription	PPR43587A
POLR2C (RNA polymerase II subunit C)	16q21	It is the third largest subunit of RNA polymerase II	PPR62584A

systems). Gene expression levels were measured with Applied Biosystems 7500 Real-Time PCR system. Amplification was conducted with SYBR green-based specific primers and Master Mix (Bio-rad, iTaq Universal SYBR Green Supermix). Glyceraldehyde-3-phosphate dehydrogenase (GAPDH) was used as the endogenous control gene (housekeeping). The $2^{-\Delta\Delta CT}$ method was used to calculate the differences between gene expressions. The primer catalog numbers and genes subjected to quantitative real-time polymerase chain reaction analysis are listed in Table 1.

Histological analysis

For histological examinations, ovarian tissues were embedded in paraffin blocks after being treated with 10% formaldehyde. Block slices of paraffin that were 5–6 mm thick were stained with hematoxylin and eosin (H&E). An experienced pathologist reviewed the preparations using an Olympus BX-50 light microscope. In each rat ovary, the first, fifth, and tenth sections were used to count the follicles and corpus luteum.

Hormone analyses

Estradiol, LH, FSH, SHBG, GnRH, ACTH, AMH, and Cortisol levels in the serum were measured using Elisa kits (Fine Biotech Co. Ltd.) according to the manufacturer's instructions. The optical density values were detected with a Multiskan™ FC Microplate Photometer (Thermo Fisher Scientific™).

Total antioxidant level and total oxidant level tests

Serum total antioxidant level (TAL), total oxidant level (TOL), and oxidative stress index (OSI) values were measured using Rel Assay brand commercial kit (Rel Assay Kit Diagnostics). Results are expressed as mmol Trolox equiv./lt. Serum TAL and TOL levels were calculated μmol H_2O_2 equiv./L. OSI, which is expressed as the ratio of TOL levels to TAL levels, was calculated. The results were expressed as "arbitrary units" (AU). OSI (AU) = TOL, μmol H_2O_2 equiv./L/TAL, mmol Tro-

lox equiv./L X10.

Statistical analyses

Statistical analyses were conducted with IBM SPSS 22.0 software licensed to Fırat University (193.255.124.131) in the study. The data obtained are presented as mean ± standard deviation. Statistical differences were calculated with one-way ANOVA tests for independent groups. $P < 0.05$ was considered statistically significant when interpreting the results.

RESULTS

Analysis of height, total weight, and ovary weight

The final weight and height of the Cisplatin ($P < 0.001$ and $P < 0.001$) and Cisplatin + AP39 ($P = 0.009$ and $P = 0.032$, respectively) groups were significantly lower than those of the control groups due to Cisplatin. The CIS group's final height was substantially greater than that of the Cisplatin ($P = 0.003$) and Cisplatin + AP39 groups ($P = 0.047$) groups. It also decreased the end weight in comparison to AP39 groups in the Cisplatin ($P = 0.001$) and Cisplatin + AP39 ($P = 0.048$) groups. The Cisplatin group's final weight was significantly lower than that of the CIS group ($P = 0.012$). Compared to the control and AP39 groups, the ovary weight was significantly lower in the Cisplatin ($P < 0.001$ and $P < 0.001$, respectively) and Cisplatin + AP39 ($P = 0.002$ and $P < 0.001$, respectively) groups. In comparison to the cisplatin and Cisplatin + AP39 groups, there were statistically significant increases in ovary weight in the CIS ($P = 0.001$ and $P = 0.01$) and CIS + AP39 ($P = 0.001$ and $P = 0.010$) groups (Fig. 2).

Change in the estrous cycle phases

Based on the diestrus and proestrus phases, there were no significant differences between the groups ($P > 0.05$). Significant decreases were observed in the AP39 ($P < 0.001$), Cisplatin ($P = 0.002$), Cisplatin + AP39 ($P < 0.001$), CIS ($P < 0.001$), and CIS + AP39 ($P = 0.001$) groups in the estrus compared to the control group. In the Cisplatin group, the metestrus phase was longer than in the control group ($P < 0.001$), and in the Cisplatin + AP39 group, the metestrus phase duration was normalized by AP39 administration ($P = 0.355$, control vs. Cisplatin + AP39) (Fig. 3).

Analysis of the forced swim test data

Immobility was found to be significantly higher in the Cisplatin and CIS groups when compared to the control group ($P < 0.001$), and in the CIS + AP39 groups, the application of AP39 normalized this increase ($P > 0.05$). The results showed that there was no discernible difference in the groups' climbing and swimming behaviors ($P > 0.05$) (Fig. 4).

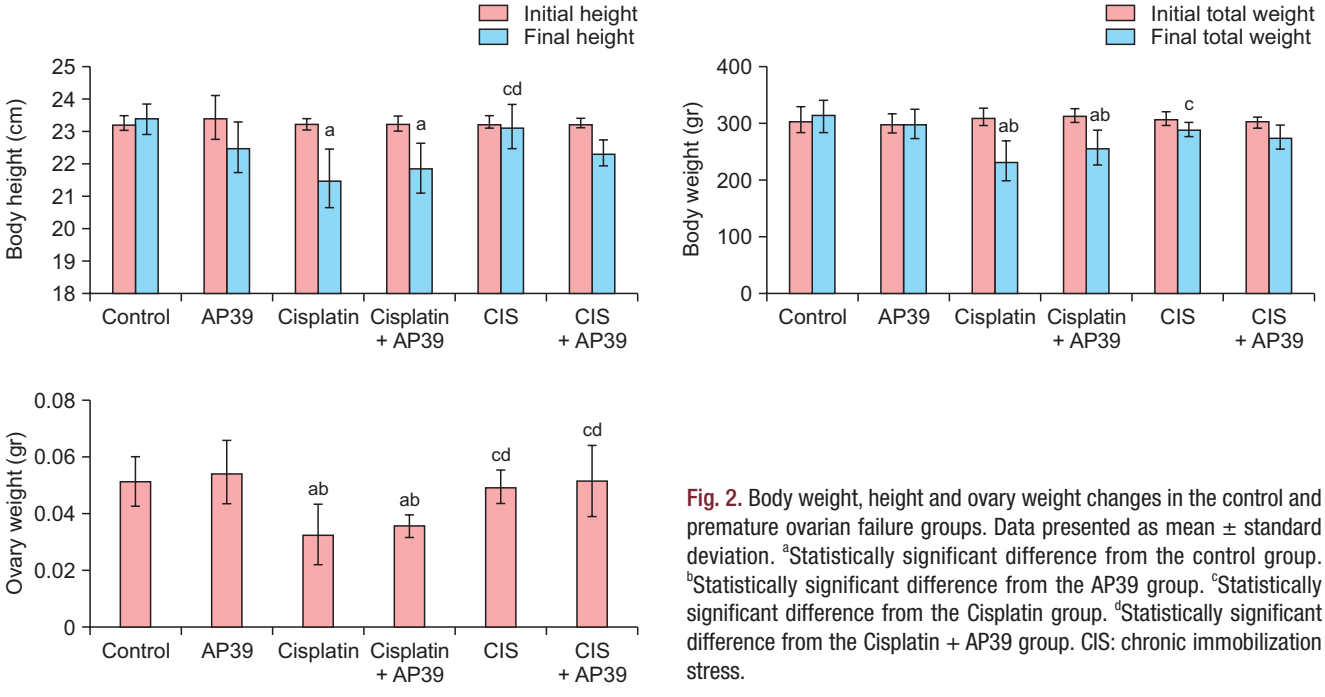

Fig. 2. Body weight, height and ovary weight changes in the control and premature ovarian failure groups. Data presented as mean ± standard deviation. [a]Statistically significant difference from the control group. [b]Statistically significant difference from the AP39 group. [c]Statistically significant difference from the Cisplatin group. [d]Statistically significant difference from the Cisplatin + AP39 group. CIS: chronic immobilization stress.

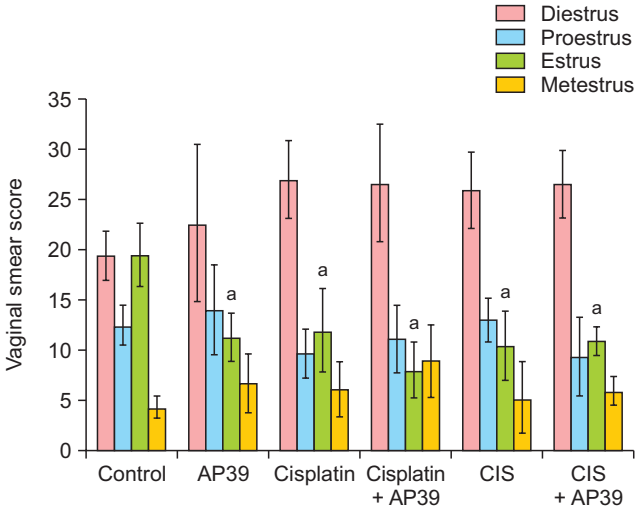

Fig. 3. Menstrual cycle phases of groups. Data presented as mean ± standard deviation. [a]Statistically significant difference from the control group. CIS: chronic immobilization stress.

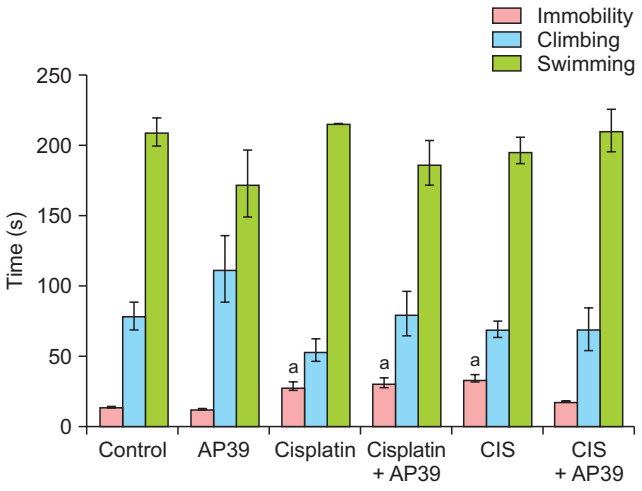

Fig. 4. Immobility, climbing and swimming times (s) of rats in forced swim test. Data presented as mean ± standard deviation. [a]Statistically significant difference from the control group. CIS: chronic immobilization stress.

Hormonal evaluation

In all research groups, there was no discernible change in serum ACTH levels ($P > 0.05$). Serum cortisol levels did not differ ($P > 0.05$) from the control group; FSH ($P = 0.013$), LH ($P = 0.003$), E2 ($P = 0.047$), SHBG ($P < 0.001$), and AMH ($P = 0.001$) levels were higher in the cisplatin group than in the control group. LH levels in the Cisplatin + AP39 group returned to normal after AP39 administration ($P = 0.74$, compared to Cisplatin + AP39 and control). GnRH, LH, and E2 levels did not alter in the CIS group relative to the control group ($P > 0.05$); FSH ($P = 0.013$) and cortisol ($P = 0.035$) increased, while SHBG ($P = 0.011$) and AMH ($P = 0.001$) decreased. Cortisol levels in the CIS + AP39 group were normalized after AP39 administration ($P = 0.65$ when comparing CIS + AP39 to control) (Fig. 5).

Analysis of quantitative real-time polymerase chain reaction data

When comparing the control group's gene expressions to those related to mitochondrial biogenesis, AP39 administration resulted in significantly higher levels of *MFN2, ATP5B, TFAM, CHRM1, OPA1,* and *NFE2L2* gene expressions and significantly lower levels of PPARGC1A and PRKAA2 gene expressions ($P < 0.05$). Compared to the control group, there was a significant decrease in the gene expressions of PPARGC1A and PRKAA2, and a significant increase in the expressions of *MFN2*, *ATP5B*, *TFAM*, *HIF1A*, and *OPA1*, *NFE2L2*, following cisplatin treatment ($P < 0.05$). Only *PPARGC1A*, *ATP5B*, and *MFN2* expression were normalized by AP39 administration in the Cisplatin + AP39 group ($P < 0.05$). Compared to the control group, the CIS protocol resulted in a significant decrease in *PPARGC1A*, *PRKAA2*, and *PPARGC1B* gene expressions and a significant increase in *MFN2*, *CHRM1*, *HIF1A*, *OPA1*, and *NFE2L2* gene expressions ($P < 0.05$). Only *MFN2* and *PPARGC1A* expression were normalized by AP39 administration in the CIS + AP39 group ($P < 0.05$). All treatment groups showed a significant increase in oogenesis-related gene expressions ($P < 0.05$) compared to the control group for *DAZL, ZP1, ZP2, NPM2, H1FOO, DNMT1, DNMT3B, KAT2A, HDAC3, SIRT7, MBD2, KMT2A, SMARCA1, ESR, MAP2K1, NCOA1, MED15,* and *POLR2C*, and a significant decrease in *DPPA-3* and *GTF2H1* gene expressions. In the cisplatin + AP39 group, AP39 administration did not normalize the expression of any gene. The only genes whose expressions were considerably lower than those of the Cisplatin group ($P < 0.05$) were *DAZL*, *NPM2*, and *NCOA1*. Conversely, it markedly elevated the expressions of *HDAC3, SIRT7, MBD2, ZP2, H1FOO, DNMT3B, KAT2A, ESR1, MAP2K1,* and *GTF2H1* ($P < 0.05$). It's interesting to note that while Ap39 treatment considerably decreased the expressions of *DAZL, ZP1, ZP2, H1FOO, HDAC3, SIRT7, MBD2, ESR1,* and *MAP2K1* in CIS+AP39 group relative to the CIS group ($P < 0.05$), it did not normalize them (Table 2).

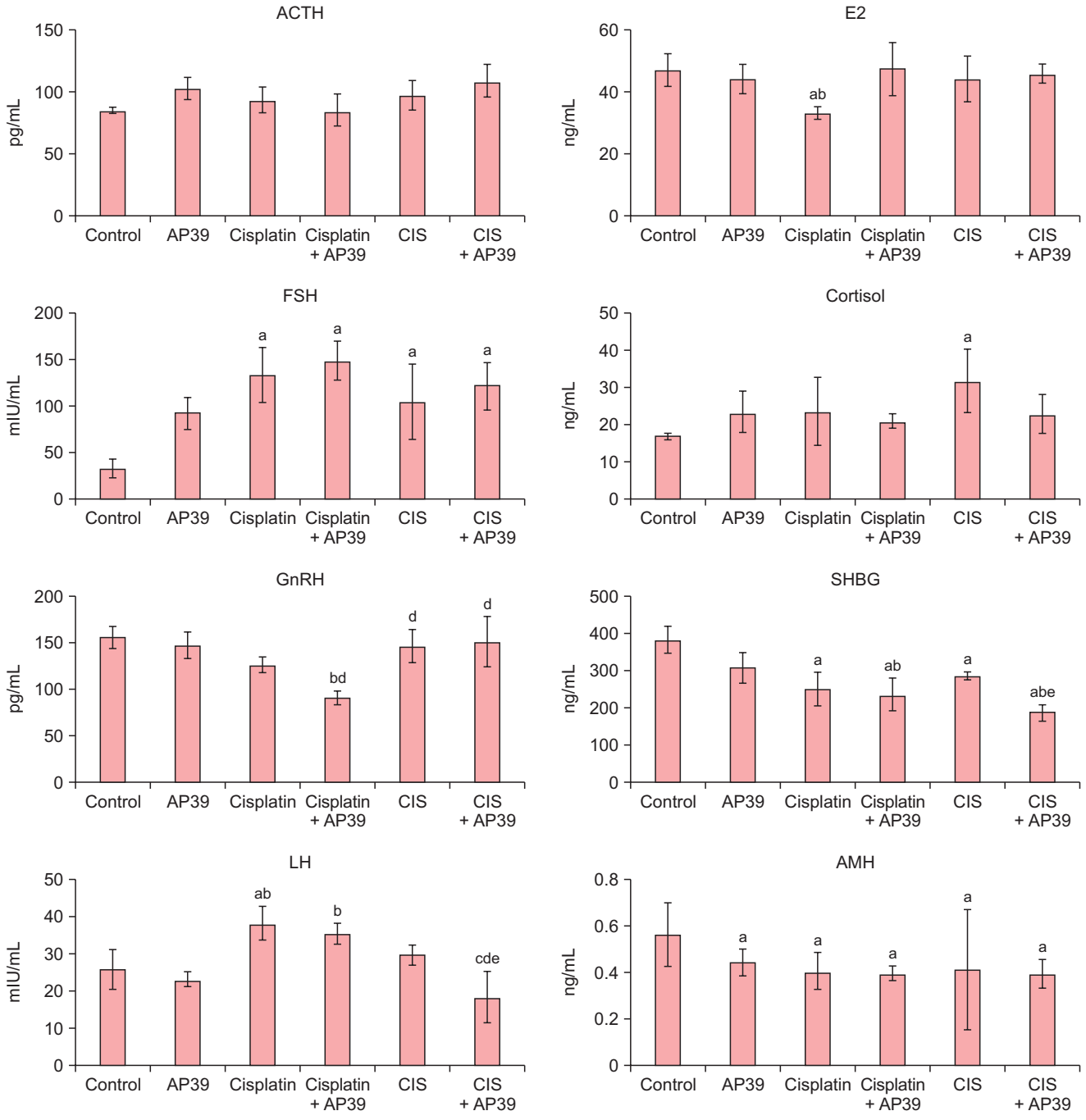

Fig. 5. Serum levels of hormones in control and premature ovarian failure groups. Data presented as mean ± standard deviation. [a]Statistically significant difference from the control group. [b]Statistically significant difference from the AP39 group. [c]Statistically significant difference from the Cisplatin group. [d]Statistically significant difference from the Cisplatin + AP39 group. [e]Statistically significant difference from the CIS group. CIS: chronic immobilization stress.

Analysis of serum total antioxidant level and total oxidant level levels

The TAL levels of the groups were found to be similar ($P > 0.05$). The intracellular TOL level were all significantly higher in Cisplatin and CIS group than the control group ($P = 0.000$ and $P = 0.003$, respectively). Normalized TOL levels were observed in the AP39-treated groups ($P = 0.095$ and $P = 0.624$, respectively,

Table 2. mRNA fold-changes in the genes analyzed with quantitative real-time polymerase chain reaction in ovary tissue

Gene	AP39		Cisplatin		Cisplatin + AP39		CIS		CIS + AP39	
	mRNA fold change	*P*	mRNA fold change	*P*	mRNA fold change	*P*	mRNA fold change	*P*	mRNA fold change	*P*
GAPDH	1	0	1	0	1	0	1	0	1	0
Mitochondrial function related genes										
MFN2	2.82[a]	0.02	3.03[a]	0.020	1.65	0.11	2.31	0.04	1.68	0.110
NRF1	1.08	0.74	0.99	0.978	0.45	0.04	1.39	0.26	0.60	0.113
ATP5B	2.42[a]	0.033	3.36[a]	0.017	1.46[c]	0.199	1.57	0.15	2.07	0.034
TFAM	2.12[a]	0.048	2.20[a]	0.043	0.67	0.187	1.96	0.06	1.13	0.651
PPARGC1A	0.06[a]	0.00	0.18[a]	0.009	0.17	0.009	0.18	0.01	0.24	0.012
CHRM1	20.82[a]	0.005	0.93[b]	0.788	0.40[bc]	0.030	8.69[b]	0.01	6.06[bd]	0.008
HIF1A	1.01	0.978	3.66[ab]	0.015	5.10[ab]	0.010	3.39[ab]	0.02	9.38[abd]	0.006
OPA1	8.34[a]	0.007	9.51[a]	0.006	4.14[bc]	0.012	6.54[b]	0.01	6.59[b]	0.008
PRKAA2	0.50[a]	0.048	0.45[a]	0.042	0.43[a]	0.038	0.40[a]	0.03	0.53	0.072
MFN1	1.19	0.514	1.12	0.651	0.63	0.138	0.83	0.48	0.71	0.240
NFE2L2	2.66[a]	0.027	2.23[a]	0.041	2.19[a]	0.044	2.62[a]	0.03	2.55[a]	0.029
PPARGC1B	1.10	0.728	0.75	0.310	0.22	0.011	0.46	0.05	0.97	0.892
Ovarian function related genes										
DPPA3	0.18[a]	0.009	0.12[a]	0.007	0.08[a]	0.006	0.10[a]	0.01	0.01[a]	0.004
FIGLA	1.71	0.104	1.49	0.181	0.31[a]	0.018	1.40[a]	0.24	1.91	0.069
DAZL	16.22[a]	0.005	15.67[a]	0.005	8.06[abc]	0.007	15.35[a]	0.01	3.46[ad]	0.016
ZP1	4.79[a]	0.010	2.00[ab]	0.038	0.45[ab]	0.042	12.82[ab]	0.01	4.06[ad]	0.013
ZP2	10.82[a]	0.006	13.36[ab]	0.006	25.99[abc]	0.005	71.51[ab]	0.00	16.11[abd]	0.005
POU5F1	1.13	0.633	0.71	0.248	0.11[a]	0.007	1.54	0.16	0.75	0.310
NPM2	13.09[a]	0.006	26.72[ab]	0.005	4.35[abc]	0.012	25.28[ab]	0.00	31.78[abd]	0.005
H1FOO	4.14[a]	0.012	3.20[a]	0.018	8.69[abc]	0.007	6.82[a]	0.01	4.96[ad]	0.010
DNMT1	11.31[a]	0.005	12.30[a]	0.006	14.72[ab]	0.006	15.89[ab]	0.01	13.83[ab]	0.006
DNMT3B	5.13[a]	0.010	5.66[a]	0.009	17.15[abc]	0.005	5.10[a]	0.01	6.19[a]	0.008
KAT2A	12.82[a]	0.006	17.27[ab]	0.005	42.22[abc]	0.005	19.70[ab]	0.01	20.97[ab]	0.005
HDAC3	10.56[a]	0.006	11.47[a]	0.006	63.12[abc]	0.004	24.08[ab]	0.00	15.24[abd]	0.005
SIRT7	12.64[a]	0.006	14.03[a]	0.006	54.95[abc]	0.005	22.94[ab]	0.00	18.50[abd]	0.005

Table 2. Continued

Gene	AP39		Cisplatin		Cisplatin + AP39		CIS		CIS + AP39	
	mRNA fold change	*P*	mRNA fold change	*P*	mRNA fold change	*P*	mRNA fold change	*P*	mRNA fold change	*P*
MBD2	8.00[a]	0.007	10.56[ab]	0.006	114.56[abc]	0.004	15.67[ab]	0.01	3.51[abd]	0.016
KMT2A	2.53[a]	0.030	3.71[a]	0.014	4.59[ab]	0.011	3.89[a]	0.01	2.54[a]	0.030
SMARCA1	2.40[a]	0.034	1.18	0.530	2.89[ac]	0.022	2.25[a]	0.04	1.60	0.134
ESR1	82.71[a]	0.004	78.25[a]	0.004	221.32[abc]	0.004	380.04[ab]	0.00	124.50[abd]	0.004
MAP2K1	99.73[a]	0.004	116.97[ab]	0.004	130.69[abc]	0.004	187.40[ab]	0.00	77.71[abd]	0.004
NCOA1	2.00[a]	0.039	1.87	0.074	0.13[abc]	0.007	0.13[ab]	0.01	0.73[bd]	0.264
TBP	0.52	0.069	0.30[a]	0.017	0.24[a]	0.012	0.10[a]	0.01	0.15[a]	0.007
POLR2C	4.99[a]	0.01	4.89[a]	0.010	4.40[a]	0.014	3.65[a]	0.014	4.19[a]	0.012
GTF2H1	0.25[a]	0.01	0.16[ab]	0.01	3.27[abc]	0.017	0.18[a]	0.009	0.16[a]	0.008

Data presented as mean ± standard deviation.
CIS: chronic immobilization stress.
[a]Statistically significant difference from the control group.
[b]Statistically significant difference from the AP39 group.
[c]Statistically significant difference from the Cisplatin group.
[d]Statistically significant difference from the CIS group. $P < 0.05$: versus control group.

for control versus CIS + cisplatin and CIS + AP39) (Fig. 6).

Immunohistochemical data analysis

Examination using light microscopy revealed that the ovarian tissues in the control group had a normal appearance. In the control group, all phases of follicular development were noted. A similar histopathological appearance was observed to POF ovary appearance in cisplatin and CIS groups. Comparing the AP39, Cisplatin, and CIS groups to the control group, significant increases in stromal cellularity (black asterisk) and degeneration in follicular epithelial cells (red arrow) were noted. Neither the CIS nor the Cisplatin groups showed any appreciable histological alterations. In contrast to the cisplatin and CIS groups, the AP39 treatment group showed a minimal reduction in histopathological alterations (Fig. 7).

The evaluation of primordial follicle numbers in the experimental groups revealed a significant decrease in all groups compared to the control group ($P = 0.000$). While the cisplatin group showed a significant decrease ($P = 0.024$) compared to the Ap39 group, this significance was not observed in the other groups ($P > 0.05$). The study found a significant increase in the number of primordial follicles in the CIS groups compared to the

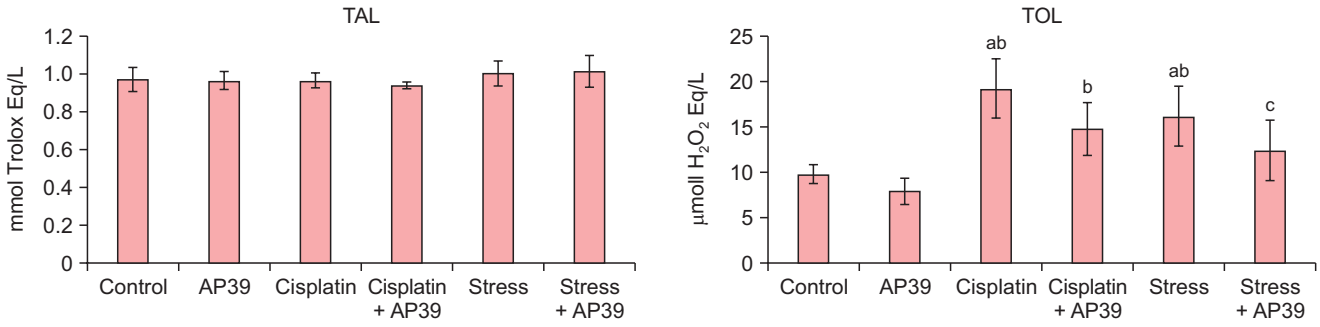

Fig. 6. Serum TAL and TOL levels in study groups. [a]Statistically significant difference from the control group. [b]Statistically significant difference from the AP39 group. [c]Statistically significant difference from the Cisplatin group. TAL: total antioxidant level, TOL: total oxidant level.

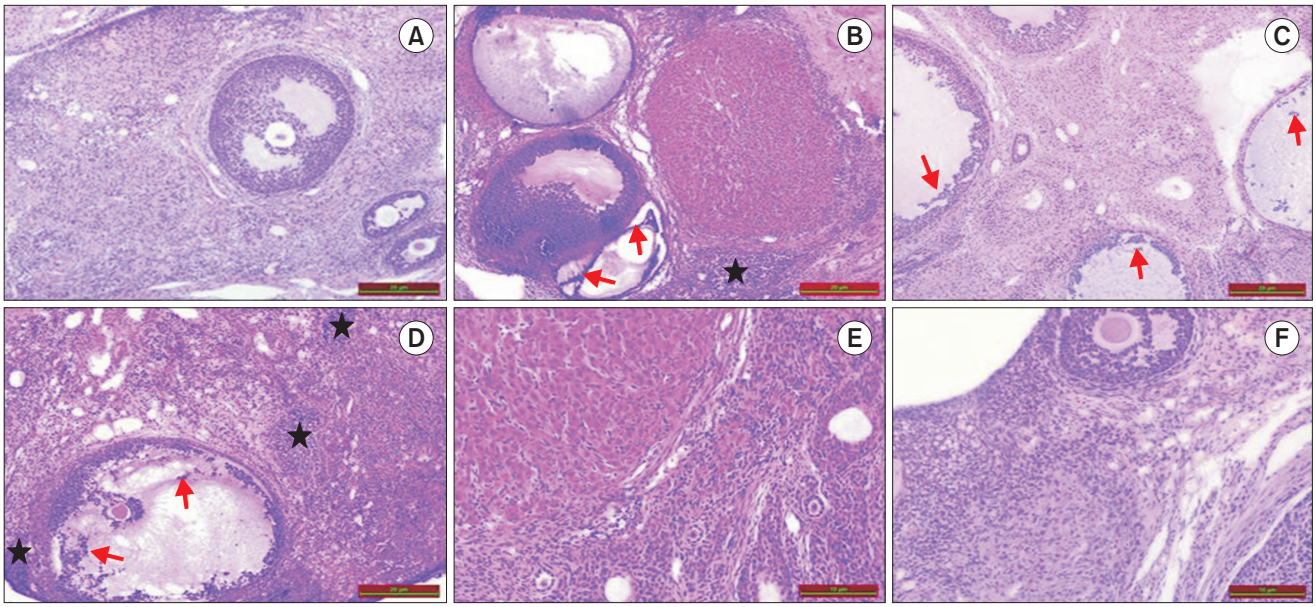

Fig. 7. Histology of the ovaries from control and premature ovarian failure groups. All sections were stained with hematoxylin and eosin (H&E, ×20). ★: increased stromal cellularity, →: degeneration of follicular epithelial cells. (A) Control, (B) Cisplatin, (C) CIS, (D) AP39, (E) Cisplatin + AP39, (F) CIS + AP39. CIS: chronic immobilization stress.

Table 3. Effect of AP39 on follicular development in cisplatin and CIS-induced ovarian injury

Folliculogenesis stage	Group					
	Control	AP39	Cisplatin	Cisplatin + AP39	CIS	CIS + AP39
Primordial follicle	6.57 ± 0.78	4.14 ± 0.69[a]	2.42 ± 0.97[a]	3.14 ± 0.69[a]	4.42 ± 0.97[a]	4.00 ± 0.81[a]
Developing follicle	13.57 ± 1.72	8.57 ± 1.13[a]	5.71 ± 1.49[ab]	7.71 ± 2.05[ab]	9.17 ± 1.16[a]	8.00 ± 1.73[a]
Atretic follicle	0.42 ± 0.53	1.21 ± 0.75	2.14 ± 3.77[a]	1.57 ± 0.53[a]	1.28 ± 0.48	1.28 ± 0.48
Corpus luteum	10.42 ± 0.97	10.71 ± 1.11	10.73 ± 1.13	10.45 ± 1.15	10.57 ± 1.27	10.42 ± 0.97

Data presented as mean ± standard deviation.
CIS: chronic immobilization stress.
[a]Statistically significant difference from the control group.
[b]Statistically significant difference from the AP39 group.

cisplatin group ($P = 0.005$ and $P = 0.048$). Additionally, a significant decrease in the number of developing follicles was observed in all groups compared to the control ($P = 0.000$). However, the CIS + AP39 group showed a significant increase in the number of developing follicles compared to the cisplatin group. The study found a significant increase in the number of atretic follicles in both the cisplatin and cisplatin + AP39 groups compared to the control group ($P = 0.00$ and $P = 0.019$, respectively). However, there was no statistically significant difference in the number of corpus luteum among the experimental groups ($P = 0.98$). Effect of AP39 on follicular development in cisplatin and CIS-induced ovarian injury was represented in Table 3.

DISCUSSION

Today, gonadotoxicity from long-term chemotherapy or stress exposure has become important cause of POF [21,22]. Psychological stress can impair female reproductive and endocrine functions through the hypothalamic-pituitary-adrenal (HPA) and hypothalamus-pituitary-ovarian (HPO) axis, leading to decreased ovarian reserve [23]. In rodent models of POF, which is characterized by low levels of gonadal hormones such as estrogens and AMH, and high levels of gonadotropins such as FSH and LH, the assessment index can be established by combining simple estrous cycle monitoring with analysis of serum hormones, including E2, AMH, and FSH, and histological follicle counts [24]. In the present study, cisplatin and CIS-treated rats revealed that the estrus cycle, HPO axis hormonal network, mitochondrial biogenesis, and egg quality-related gene expressions related to the process of folliculogenesis were impaired, application of CIS also disrupted HPA axis and long-term AP39 (0.3 mg/kg/day) administaration, as a mitochondrial protective supplement, had limited healing properties in both models.

An ideal animal model; has pathogenic pathways and processes similar to those observed in humans, pathological changes in the model are reversible with drugs, and results must be reproducible. As expected, our 55-day CIS regimen in rats produced anxiety and depression-like behaviors in the FST, which is consistent with other research assessing the utility of CIS as a POF model [20,25]. Current CIS model has both advantages and disadvantages. On the positive side, the modeling method is consistent with the primary pathogenic factors of human POF, including increased FSH and decreased AMH, prolonged estrous cycle characterized by a decrease in the estrus count and the decrease of follicle counts. Additionally, the CIS modeling method is simple and feasible. Compared to CUMS, CIS reduces the workload of the staff as it is easy to implement. On the negative side, the CIS model does not meet the criteria for use as a POF model due to decreased E2 and increased LH, but it does exhibit all other POF characteristics, such as prolonged estrous cycle and decreased number of primordial and developing follicles. Therefore, it is suitable for use as a model of ovarian dysfunction, but not POF.

Recent studies on restraint stress and CUMS rodent models of POF have reported decreases in serum levels of AMH, E2, and GnRH, as well as increases in progesterone, FSH, and LH levels. These changes were accompanied by prolongation of the estrous cycle and decrease in follicle numbers [17,21,26,27]. The main cause of our current CIS protocol's failure to meet one of the POF model's essential hormonal requirements—E2 reduction and LH rise—is the incomplete understanding of how various CIS protocols affect the HPA

and HPO axis in rats. Specifically, administration of CIS for 3 hours a day for 28 days led to a decrease in FSH and LH secretion [28], while administration for 6 hours a day for 15 days resulted in an increase in FSH, prolactin, and cortisol, and a decrease in LH, estrogen, and progesterone [29]. Additionally, short-term application of CIS for 45 minutes a day for 7 days was found to decrease LH and FSH levels [30]. Our study utilized a longer CIS procedure, lasting only 1–3 hours per day, for a total of 55 days with increasing durations. Although our CIS POF model showed an increase in FSH and a decrease in SHBG and AMH, similar to the restraint stress and CUMS POF stress models, we did not observe a decrease in E2 or an increase in LH when evaluated in terms of the HPO axis. To use CIS as a POF model, standardized protocols are necessary to observe hormonal axis changes.

Consistent with previous cisplatin POF model studies, intraperitoneal cisplatin injections (3 mg/kg/day) for at least 10 days caused a decrease in ovarian reserve by reducing the number of primordial and developing follicles with a decrease in E2 and an increase in FSH and prolonged estrous cycle characterized by a decrease in the estrus count [17,19,31]. Cisplatin also significantly prolonged FST immobilization times and caused significant reductions in height, weight, and ovarian weight, which are in line with previous research [32,33]. AP39 administration not normalized these deteriations. Although cisplatin has been shown to cause more serious disruptions in the estrous cycle than CIS, we have detected a prolonged estrous cycle in all treatment groups. In several studies conducted with rodent cisplatin-induced POF models, increased FSH, LH, and ACTH hormone levels and diminished E2, SHBG, and AMH hormone levels were reported [5,22,34-36]. The present study revealed that the cisplatin POF model had not changed in GnRH, ACTH, and cortisol levels, the increased FSH and LH, and the diminished E2, SHBG, and AMH levels. The AP39 normalized only LH levels in the Cisplatin-treated animals. Supporting our hormonal findings, we observe significant increases histopathologically in stromal cellularity, degeneration in follicular epithelial cells and reduction of ovarian reserve in AP39, cisplatin. Administration of AP39 resulted in a little improvement in follicle reserve, estrus cycle deteriorations, and histopathological abnormalities.

It has been reported that in animal models, cisplatin and stress significantly increase malondialdehyde levels as an end product of lipid peroxidation, in addition to its ability to inhibit the activity of antioxidant enzymes in ovarian tissue [36,37]. Although TOL analyses were not performed directly on the ovarian tissue, it was shown that cisplatin and CIS applications significantly increased serum TOL levels, and the application of AP39, an antioxidant compound, normalized this increase. The present study suggests that one of the main biochemical mechanisms underlying this healing effect of AP39 in both models may be to normalize by oxidative stress levels. However, prolonged usage of large dosages of AP39 is believed to be one of the primary causes of the partial healing qualities. The administration of 0.3 mg/kg/day AP39 alone in healthy rats also disrupted mitochondrial biogenesis and oogenesis with a possible dose dependent-toxic effect. The dose of AP39 administered in our study was determined according to the study of Ahmad et al. [13] in which the curative effects of a short-term administration of AP39 (0.1, 0.2, and 0.3 mg/kg) at a dose of 0.3 mg/kg for 6 hours during reperfusion in a rat acute kidney injury model were shown [13]. Regarding the curative effects of AP39, there are two studies similar to our study but using lower doses for a longer period of time. Administration of 100 nM/kg/day of AP39 to APP/PS1 mice for 6 weeks was shown to significantly ameliorate spatial memory deficits in the Morris water maze, reduce Aβ accumulation in their brains, and inhibit brain atrophy [8]. Daily administration of AP39 (0.05 or 0.1 mg/kg/day) for 7 weeks improved activity scores of non-alcoholic fatty liver disease by reducing lipid accumulation, oxidative stress, and mitochondrial dysfunction in a rat high-fat diet model [38]. In the current study, it is thought that one of the mechanisms underlying AP39's disruption of mitochondrial biogenesis and oogenesis in healthy rats and its limited curative properties may be due to the toxic effects of AP39 due to long-term use at a high dose of 0.3 mg/kg. However, in a recent study to support our data, it was shown that exposure of neurons to 100 nM AP39 significantly increased basal oxygen consumption rate, mitochondrial activity, and energy production, while 250 nM dose caused a decrease in these parameters. These data demonstrate that AP39 has biphasic effects on cellular bioenergetics and acts as an additional bioenergetic stimulant at low concentrations. However, it has been determined that it has toxic effects on the contrary at high doses [8]. In our study, we also found that high doses of AP39 resulted in significant fold changes in oogenesis gene expression

levels, indicating toxic effects. To further understand the molecular mechanisms behind these adverse effects, it is necessary to determine the LC50 and LD50 doses of the molecule for long-term use. Although the mechanism of toxicity of H_2S is still not fully known, it is known that possible mechanisms include mitochondrial dysfunction, inflammation and increased apoptosis due to overload of mitochondria with H_2S [39]. Therefore, lower doses would be appropriate for long-term use of AP39, and, in this sense, the mechanisms underlying the toxic effects of AP39 at high doses will be elucidated.

Several studies demonstrated that mitochondrial, oocyte quality, and folliculogenesis dysfunction is associated with diseases characterized by ovarian tissue damage or atresia, in human POF or rat models and knockout mice [3,7,40,41]. In the present study, in ovary tissues of AP39, CIS, and cisplatin treatments generally detected similar upregulated mitochondrial biogenesis and oogenesis-related gene expression patterns, AP39 application provided significant improvement in gene expressions related to oocyte quality in cisplatin and CIS model animals, it could not achieve normalization similar to the control, it normalized the expressions of mitochondria related Mfn2 and Ppargc1β in both models. AP39 is known to increase oxidative phosphorylation and ATP synthesis in mitochondria. However, the signaling pathway it uses to enhance mitochondrial activity and its effect on mitochondrial gene expression remain unknown [9,11,42]. PGC-1α, which is encoded by PPARGC1A, activates NRF1/2 and subsequently TFAM and serves as the primary regulator of tissue adaptation to increased energy demands by controlling mitochondrial biogenesis. Meanwhile, PGC-1β, encoded by PPARGC1B, helps maintain basal mitochondrial function [42]. In the current study, PGC1-α expression decreased in all treatment groups. However, PPAR-β and downstream targets NRF-1 and TFAM remained unchanged, except for borderline changes in a few groups. This suggests that the PPAR-β/NRF-1/TFAM pathway continues to work actively due to oxidative stress all treatment groups and AP39 appears to act through PPARβ. This data supports the reduction of TWEAK-mediated PPARα, a pro-inflammatory cytokine, in oxidative tissue damage states, such as renal kidney injury [42]. The limited therapeutic properties of AP39 at the dose we used may be due to its inability to normalize cisplatin- and CIS-induced PPARα expression, while it restores PPARβ and Mfn2 expression [43].

In conclusion, Unlike the cisplatin rats, the CIS induced ovarian dysfunction model displays a better estrus cycle, hormonal profile, and unchanged weight. AP39 administration partially ameliorates cisplatin and CIS-induced impairment in vivo. Serum E2, LH, FSH, and AMH should be used in conjunction with histological findings, molecular profile, and estrous cycle to fully reveal rodent reproductive functions. Crucially, this novel model of CIS-induced ovarian dysfunction may be utilized to investigate novel compounds' therapeutic efficacy, deteriorations linked to oogenesis, and modulation of ovarian gene expression in response to stress in vivo.

FUNDING

This work was supported by grants from the Firat University Scientific Research Unit (FUBAP, Project No: TF.17.28).

CONFLICT OF INTEREST

No potential conflict of interest relevant to this article was reported.

REFERENCES

1. Lebovic DI, Naz R. Premature ovarian failure: think 'autoimmune disorder.' Sex Reprod Menopause 2004; 2: 230-3.
2. Podfigurna-Stopa A, Czyzyk A, Grymowicz M, Smolarczyk R, Katulski K, Czajkowski K, et al. Premature ovarian insufficiency: the context of long-term effects. J Endocrinol Invest 2016; 39: 983-90.
3. Chen W, Xu X, Wang L, Bai G, Xiang W. Low expression of Mfn2 is associated with mitochondrial damage and apoptosis of ovarian tissues in the premature ovarian failure model. PLoS One 2015; 10: e0136421.
4. Jeelani R, Khan SN, Shaeib F, Kohan-Ghadr HR, Aldhaheri SR, Najafi T, et al. Cyclophosphamide and acrolein induced oxidative stress leading to deterioration of metaphase II mouse oocyte quality. Free Radic Biol Med 2017; 110: 11-8.
5. Delkhosh A, Delashoub M, Tehrani AA, Bahrami AM, Niazi V, Shoorei H, et al. Upregulation of FSHR and PCNA by administration of coenzyme Q10 on cyclophosphamide-induced premature ovarian failure in a mouse model. J Biochem Mol Toxicol 2019; 33: e22398.
6. Jang H, Na Y, Hong K, Lee S, Moon S, Cho M, et al. Synergistic effect of melatonin and ghrelin in preventing cisplatin-induced

ovarian damage via regulation of FOXO3a phosphorylation and binding to the $P27^{Kip1}$ promoter in primordial follicles. J Pineal Res 2017; 63: e12432.
7. Zhang T, Yan D, Yang Y, Ma A, Li L, Wang Z, et al. The comparison of animal models for premature ovarian failure established by several different source of inducers. Regul Toxicol Pharmacol 2016; 81: 223-32.
8. Zhao FL, Fang F, Qiao PF, Yan N, Gao D, Yan Y. AP39, a mitochondria-targeted hydrogen sulfide donor, supports cellular bioenergetics and protects against Alzheimer's disease by preserving mitochondrial function in APP/PS1 mice and neurons. Oxid Med Cell Longev 2016; 2016: 8360738.
9. Yang T, Yang Q, Lai Q, Zhao J, Nie L, Liu S, et al. AP39 inhibits ferroptosis by inhibiting mitochondrial autophagy through the PINK1/parkin pathway to improve myocardial fibrosis with myocardial infarction. Biomed Pharmacother 2023; 165: 115195.
10. Pomierny B, Krzyżanowska W, Jurczyk J, Skórkowska A, Strach B, Szafarz M, et al. The slow-releasing and mitochondria-targeted hydrogen sulfide (H_2S) delivery molecule AP39 induces brain tolerance to ischemia. Int J Mol Sci 2021; 22: 7816.
11. Magierowska K, Korbut E, Wójcik-Grzybek D, Bakalarz D, Sliwowski Z, Cieszkowski J, et al. Mitochondria-targeted hydrogen sulfide donors versus acute oxidative gastric mucosal injury. J Control Release 2022; 348: 321-34.
12. Libiad M, Vitvitsky V, Bostelaar T, Bak DW, Lee HJ, Sakamoto N, et al. Hydrogen sulfide perturbs mitochondrial bioenergetics and triggers metabolic reprogramming in colon cells. J Biol Chem 2019; 294: 12077-90.
13. Ahmad A, Olah G, Szczesny B, Wood ME, Whiteman M, Szabo C. AP39, a mitochondrially targeted hydrogen sulfide donor, exerts protective effects in renal epithelial cells subjected to oxidative stress in vitro and in acute renal injury in vivo. Shock 2016; 45: 88-97.
14. Karwi QG, Bornbaum J, Boengler K, Torregrossa R, Whiteman M, Wood ME, et al. AP39, a mitochondria-targeting hydrogen sulfide (H_2S) donor, protects against myocardial reperfusion injury independently of salvage kinase signalling. Br J Pharmacol 2017; 174: 287-301.
15. Liu M, Li Z, Liang B, Li L, Liu S, Tan W, et al. Hydrogen sulfide ameliorates rat myocardial fibrosis induced by thyroxine through PI3K/AKT signaling pathway. Endocr J 2018; 65: 769-81.
16. Li Y, Liu M, Song X, Zheng X, Yi J, Liu D, et al. Exogenous hydrogen sulfide ameliorates diabetic myocardial fibrosis by inhibiting cell aging through SIRT6/AMPK autophagy. Front Pharmacol 2020; 11: 1150.
17. Fu XY, Chen HH, Zhang N, Ding MX, Qiu YE, Pan XM, et al. Effects of chronic unpredictable mild stress on ovarian reserve in female rats: feasibility analysis of a rat model of premature ovarian failure. Mol Med Rep 2018; 18: 532-40.
18. Şahin Z, Özkürkçüler A, Koç A, Solak H, Koca RÖ, Cakan P, et al. An evaluation of the effects of two chronic immobilization stress protocols on depression/anxiety- related behavior in male rats. Acıbadem Üniversitesi Sağlık Bilimleri Dergisi 2019; 3: 535-41.
19. Xu M, Sun J, Wang Q, Zhang Q, Wei C, Lai D. Chronic restraint stress induces excessive activation of primordial follicles in mice ovaries. PLoS One 2018; 13: e0194894.
20. Mao Y, Xu Y, Yuan X. Validity of chronic restraint stress for modeling anhedonic-like behavior in rodents: a systematic review and meta-analysis. J Int Med Res 2022; 50: 3000605221075816.
21. Keremu A, Yaoliwasi A, Tuerhong M, Kadeer N, Heyi, Yiming A, et al. Research on the establishment of chronic stress-induced premature ovarian failure the rat model and effects of Chinese medicine Muniziqi treatment. Mol Reprod Dev 2019; 86: 175-86.
22. Li D, Chen Y, Qi L, Ju X, Liu H, Wang G. Differentially expressed genes in cisplatin-induced premature ovarian failure in rats. Anim Reprod Sci 2013; 137: 205-13.
23. Ferlazzo A, Cravana C, Fazio E, Medica P. The contribution of total and free iodothyronines to welfare maintenance and management stress coping in Ruminants and Equines: physiological ranges and reference values. Res Vet Sci 2018; 118: 134-43.
24. Beck-Peccoz P, Persani L. Premature ovarian failure. Orphanet J Rare Dis 2006; 1: 9.
25. Şahin Z, Özen Koca R, Solak H, Özkürkçüler A, Koç A, Kalkan ÖF, et al. Comparison of the effects of immobilization stress and chronic mild stress models on depression-related behaviors in female rats: an assessment of a 10-day stress period. Fırat Üniversitesi Sağlık Bilimleri Tıp Dergisi 2019; 33: 153-7.
26. Everds NE, Snyder PW, Bailey KL, Bolon B, Creasy DM, Foley GL, et al. Interpreting stress responses during routine toxicity studies: a review of the biology, impact, and assessment. Toxicol Pathol 2013; 41: 560-614.
27. Liang B, Wei DL, Cheng YN, Yuan HJ, Lin J, Cui XZ, et al. Restraint stress impairs oocyte developmental potential in mice: role of CRH-induced apoptosis of ovarian cells. Biol Reprod 2013; 89: 64.
28. Fotsing D, Ngoupaye GT, Ouafo AC, Njapdounke SKJ, Kenneth YA, Ngo Bum E. Effects of *Gladiolus dalenii* on the stress-induced behavioral, neurochemical, and reproductive changes in rats. Front Pharmacol 2017; 8: 685.
29. Abdel-Fattah MD. Effects of immobilization stress on some reproductive functions in adult female albino rats. Med J Cairo Univ 2018; 86: 2457-62.
30. Sahin Z, Ozkurkculer A, Kalkan OF, Bulmus FG, Bulmus O, Kutlu S. Gonadotropin levels reduced in seven days immobilization stress-induced depressive-like behavior in female rats. J Basic Clin Physiol Pharmacol 2021; 33: 199-206.
31. Lovick TA. Estrous cycle and stress: influence of progesterone on the female brain. Braz J Med Biol Res 2012; 45: 314-20.

32. Zhou D, Tan RJ, Lin L, Zhou L, Liu Y. Activation of hepatocyte growth factor receptor, c-met, in renal tubules is required for renoprotection after acute kidney injury. Kidney Int 2013; 84: 509-20.
33. Abdelkader NF, Saad MA, Abdelsalam RM. Neuroprotective effect of nebivolol against cisplatin-associated depressive-like behavior in rats. J Neurochem 2017; 141: 449-60.
34. Bernardi F, Hartmann B, Casarosa E, Luisi S, Stomati M, Fadalti M, et al. High levels of serum allopregnanolone in women with premature ovarian failure. Gynecol Endocrinol 1998; 12: 339-45.
35. Yuemaier M, Tuerhong M, Keremu A, Kadeer N, Aimaiti A, Wushouer X, et al. Research on establishment of abnormal phlegmatic syndrome with premature ovarian failure rat model and Effects of Balgham Munziq treatment. Evid Based Complement Alternat Med 2018; 2018: 3858209.
36. Divyashree S, Yajurvedi HN. Long-term chronic stress exposure induces PCO phenotype in rat. Reproduction 2016; 152: 765-74.
37. Ibrahim MA, Albahlol IA, Wani FA, Abd-Eltawab Tammam A, Kelleni MT, Sayeed MU, et al. Resveratrol protects against cisplatin-induced ovarian and uterine toxicity in female rats by attenuating oxidative stress, inflammation and apoptosis. Chem Biol Interact 2021; 338: 109402.
38. Yu Y, Ye SM, Liu DY, Yang LQ. AP39 ameliorates high fat diet-induced liver injury in young rats via alleviation of oxidative stress and mitochondrial impairment. Exp Anim 2021; 70: 553-62.
39. Jiang J, Chan A, Ali S, Saha A, Haushalter KJ, Lam WL, et al. Hydrogen sulfide--mechanisms of toxicity and development of an antidote. Sci Rep 2016; 6: 20831.
40. Falender AE, Shimada M, Lo YK, Richards JS. TAF4b, a TBP associated factor, is required for oocyte development and function. Dev Biol 2005; 288: 405-19.
41. Venkatesh S, Kumar M, Sharma A, Kriplani A, Ammini AC, Talwar P, et al. Oxidative stress and ATPase6 mutation is associated with primary ovarian insufficiency. Arch Gynecol Obstet 2010; 282: 313-8.
42. Fontecha-Barriuso M, Martin-Sanchez D, Martinez-Moreno JM, Monsalve M, Ramos AM, Sanchez-Niño MD, et al. The role of PGC-1α and mitochondrial biogenesis in kidney diseases. Biomolecules 2020; 10: 347.
43. Filadi R, Pendin D, Pizzo P. Mitofusin 2: from functions to disease. Cell Death Dis 2018; 9: 330.